

Retraction

Retracted: Wireless Radio Frequency Automation of Intelligent Optical Fiber Transmission System Based on the Differential Evolution Method

Advances in Multimedia

Received 15 August 2023; Accepted 15 August 2023; Published 16 August 2023

Copyright © 2023 Advances in Multimedia. This is an open access article distributed under the Creative Commons Attribution License, which permits unrestricted use, distribution, and reproduction in any medium, provided the original work is properly cited.

This article has been retracted by Hindawi following an investigation undertaken by the publisher [1]. This investigation has uncovered evidence of one or more of the following indicators of systematic manipulation of the publication process:

- (1) Discrepancies in scope
- (2) Discrepancies in the description of the research reported
- (3) Discrepancies between the availability of data and the research described
- (4) Inappropriate citations
- (5) Incoherent, meaningless and/or irrelevant content included in the article
- (6) Peer-review manipulation

The presence of these indicators undermines our confidence in the integrity of the article's content and we cannot, therefore, vouch for its reliability. Please note that this notice is intended solely to alert readers that the content of this article is unreliable. We have not investigated whether authors were aware of or involved in the systematic manipulation of the publication process.

Wiley and Hindawi regrets that the usual quality checks did not identify these issues before publication and have since put additional measures in place to safeguard research integrity.

We wish to credit our own Research Integrity and Research Publishing teams and anonymous and named external researchers and research integrity experts for contributing to this investigation.

The corresponding author, as the representative of all authors, has been given the opportunity to register their

agreement or disagreement to this retraction. We have kept a record of any response received.

References

- [1] L. Jin, J. Zhao, X. Huang, and B. Lu, "Wireless Radio Frequency Automation of Intelligent Optical Fiber Transmission System Based on the Differential Evolution Method," *Advances in Multimedia*, vol. 2021, Article ID 1802001, 8 pages, 2021.

Research Article

Wireless Radio Frequency Automation of Intelligent Optical Fiber Transmission System Based on the Differential Evolution Method

Lei Jin , Jinghong Zhao , Xing Huang , and Bin Lu 

State Grid Liaoning Information and Communication Company, Shenyang, China

Correspondence should be addressed to Lei Jin; 201430730103@stu.scau.edu.cn

Received 1 September 2021; Accepted 22 October 2021; Published 9 December 2021

Academic Editor: Kang Song

Copyright © 2021 Lei Jin et al. This is an open access article distributed under the Creative Commons Attribution License, which permits unrestricted use, distribution, and reproduction in any medium, provided the original work is properly cited.

With the continuous development and improvement of science and technology, optical fiber transmission has been transformed from traditional manual transmission to automatic transmission, and the transmission efficiency is constantly improving. In order to further analyze the performance of the intelligent optical fiber transmission process, the differential evolution analysis method is introduced in this paper, integrated architecture is built through the integrated optical and intelligent optical fiber, and the corresponding vector signal error value is solved through the comparison of transmission schemes. The error value is about 9%, through simulation experiments, which can effectively meet the requirement of automation of the wireless radio frequency of the intelligent optical fiber transmission system and realize long-distance transmission.

1. Introduction

With the continuous development of social economy, there has been a full development in both hardware and software for data transmission, for example, from the perspective of hardware, the latest technologies such as smart optical fiber and software technologies such as radio frequency technology, while the content of transmission has also changed from the most primitive data, images, voice, and video to diverse multimedia [1–3]. In terms of the current transmission hardware, for example, copper wire can be used to meet the transmission and corresponding capacity of communication [4–6]; solutions such as high reliability, fast transmission, and low cost can be realized. Compared with traditional access methods, the smart optical fiber access can be used for a lower maintenance cost and a lower update frequency [7, 8]. Meanwhile, due to the physical characteristics of optical fiber, the communication transmission distance covered by it is also longer.

The so-called wireless radio frequency transmission uses light as the relevant carrier and converts the photoelectric data into the radio frequency signal in the transmission bandwidth signal in the optical fiber. This is a new type of transmission method with low cost, low loss, and long

transmission distance. Such transmission mode has gradually become the main method of communication transmission. According to the technical content, wireless radio frequency transmission can be divided into two types: analog and digital [9, 10].

For wireless communication or light communication, the processing, transmission, and management of information cannot be completed alone [11]. Therefore, in view of these shortcomings, key technical support is performed for the network fusion process on the basis of the fusion of optical fiber communication and wireless communication fusion relying on the differential evolution method; radio frequency automation is introduced and evaluated, aiming to lay a theory for communication base.

2. Intelligent Optical Fiber Network Construction

The intelligent optical fiber network mainly includes two parts: optical fiber access and wireless access. The wireless access mainly implements voice services through the 5G network. For optical fiber access, in the entire network architecture, all users share a single optical signal. The signal is distributed through the light source signal, but because

multiple terminal users share the entire wavelength, the cost is also reduced and maintenance is facilitated [12].

The mathematical model for the intelligent optical fiber network construction is shown in Figure 1. The transmitter of the vector signal first generates the corresponding signal and meanwhile outputs the corresponding signal-to-noise ratio index to express the quantitative calculation and calibration of the vector signal generator's noise and signal.

2.1. VSG. The system sampling frequency/s depends on the sum of the maximum and minimum frequencies of the RF signal $x_{i,t}^j = x_{\min}^j + \text{rand}(0, 1) * (x_{\max}^j - x_{\min}^j)$ and \Rightarrow . The conditions for no aliasing during the sampling process are as follows: $v_{i,t}^j$, where $x_{i,t}^j$, and the function $u_{i,t}^j$ represents the

largest integer not greater than x . When the symbol rate is $(x_{i,t}^j, v_{i,t}^j)$, the complex amplitude of the QAM signal can be obtained by the following formula:

$$s(t) = \text{Re} \left[\sum_i b(t - iT) (A_i e^{j\phi_i}) (A e^{j\omega_c}) \right] x. \quad (1)$$

Among them, \Rightarrow , $f(u_{i,t}) < f(x_{i,t})$, $x_{i,t} \leftarrow u_{i,t}$. $f(x_{i,t}) < f(\Delta)$, and $\Delta \leftarrow x_{i,t}$ are the amplitude and phase of the i -th character, respectively, $b(t)$ is the signal pulse of unit amplitude, A is the amplitude of the RF carrier, T is the character duration, $x_{i,t} \leftarrow x_{i,t}$ is the angular frequency of the carrier. The frequency response of the pulse shaping filter can be obtained by the following formula:

$$G(f) = \begin{cases} 1, & |f| < f_N(1 - \alpha), \\ \sqrt{\frac{1}{2} + \frac{1}{2} \sin \frac{\pi}{2f_N} \left[\frac{f_N - |f|}{\alpha} \right]}, & f_N(1 - \alpha) \leq |f| \leq f_N(1 + \alpha), \\ 0, & |f| > f_N(1 + \alpha). \end{cases} \quad (2)$$

In the formula, $f_N = 1/(2T)$ WiMAX standard RF carrier frequency $f_c = 2.475$ GHz, the bandwidth is 20 MHz, and the guard band bandwidth on both sides is 15 MHz each, so the total bandwidth of the RF carrier is 50 MHz. n_z (3): the value range of n_z is 1~50. In this paper, $n_z = 40$, the sampling frequency is $f_s = 125$ MS/s. The band-pass signal is sampled out of band, and noise will enter the Nyquist area. The description of the band-pass signal noise is based on the assumption that both VSG in-band and out-of-band noise come from thermal noise. Thermal noise is a Gaussian process with a mean value of 0. The noise power $P_N = n_z f_s N_0$, where $N_0 = kT/2$, the VSG output signal-to-noise ratio can be calculated by the following formula:

$$\text{SNR}_{\text{VSG}} = 10 \lg \left(\frac{P_S}{P_N} \right) = 10 \lg \left(\frac{P_S}{n_z f_s N_0} \right). \quad (3)$$

2.2. ADC. Aperture and clock jitter will reduce the signal-to-noise ratio of the ADC. The jitter noise is approximately a Gaussian process with a mean value of 0. Assuming the input signal $s(t) = s_0 \sin(2\pi f_c t)$, the signal change rate $ds/dt = 2\pi f_c s_0 \cos(2\pi f_c t)$, amplitude value is divided by $\sqrt{2}$ to get the root mean square value of ds/dt : $(ds/dt)_{\text{rms}} = 2\pi f_c s_0 / \sqrt{2}$. Let Δs_{rms} be the root mean square noise, Δt is the standard deviation $\sigma_{\text{jn,ADC}}$ of the root mean square jitter, and substituting it into the above formula to obtain $(\Delta s_{\text{rms}} / \sigma_{\text{jn,ADC}}) = (2\pi f_c s_0 / \sqrt{2})$, so that the root mean square noise obtained by the ADC is $\Delta s_{\text{rms}} = 2\pi f_c s_0 \sigma_{\text{jn,ADC}} / \sqrt{2}$. The root mean square value of the full-scale input sine wave is $s_0 / \sqrt{2}$. Therefore, the ratio of the rms signal to the rms noise is calculated to obtain the

signal-to-noise ratio between ADC noise and signal [13], as shown in the following formula:

$$\text{SNR}_{\text{jn,ADC}} = -20 \lg \left(\frac{\Delta s_{\text{rms}}}{s_0 / \sqrt{2}} \right) = -20 \lg (2\pi f_c \sigma_{\text{jn,ADC}}). \quad (4)$$

Different from jitter noise, there is still quantization noise in the binary digital output of ADC, and it is related to the influence on the signal-to-noise ratio and carrier factor [14]. The specific calculation is shown in the following formula:

$$\text{SNR}_{\text{qn,ADC}} = 6.02n + 10 \lg 3 - 10 \lg \text{PAR}. \quad (5)$$

In the formula $\text{PAR} = [\max |s(t)| / P_{\text{avg}}]^2$ ($0 \leq t \leq T$), it is related to the encoding format. For the WiMAX standard, $\text{PAR}_{\text{WiMax}} = 3(\sqrt{M} - 1) / (\sqrt{M} + 1)$.

2.3. Fiber Link. For fiber link, thermal noise is one of the important factors affecting the output error code. For the error rate of optical links, formula (6) can be used to calculate

$$\text{BER} = \exp \left(\frac{-Q^2/2}{\sqrt{2\pi}Q} \right), \quad Q \geq 3. \quad (6)$$

The noise power $P_N = (4V_{\text{max}}^2 (2^{2n} - 1) / (3 \times 2^{2n})) \text{BER}$ caused by the error code of the optical fiber link, where V_{max} is the maximum voltage of the sampled signal. The power $P_{\text{DP}} = 10 \lg [1 + |D| z B_r^2 \lambda^2 / c]$ is caused by the optical fiber dispersion, and the signal-to-noise ratio of the optical fiber link is shown in the following formula:

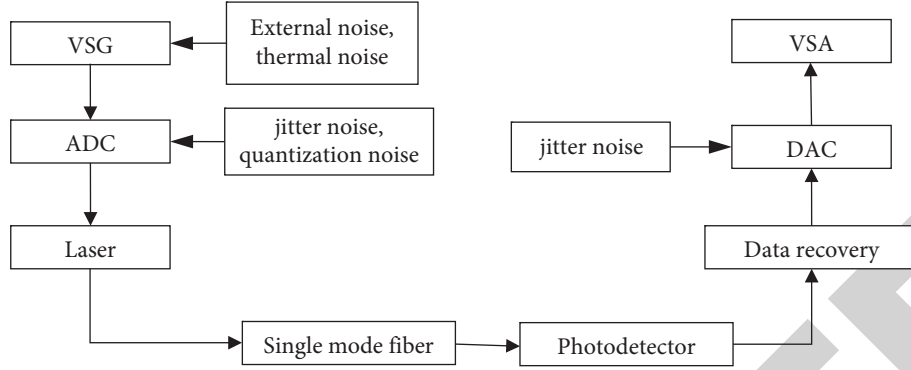


FIGURE 1: Mathematical model of digital ROF system.

$$\text{SNR}_{\text{OL}} = 10\lg \left[\frac{2^{2n} - 1}{1 + 4 \text{BER}(2^{2n} - 1)} \right] \approx 10\lg(2^{2n} - 1). \quad (7)$$

2.4. DAC. DAC clock jitter noise is a Gaussian process with an average value of 0, and the resulting signal-to-noise ratio [15] is shown in the following formula:

$$\text{SNR}_{\text{DAC}} = 10\lg \left[\left(2\pi\sigma_{\text{jn,DAC}}f_c \right)^{-2} \left(\sin c \left(\frac{f_c}{f_{\text{CLK}}} \right) \right)^{-2} \right], \quad (8)$$

where f_{CLK} is the sampling clock frequency and $\sigma_{\text{jn,DAC}}$ is the standard deviation of the root mean square jitter noise of the DAC.

2.5. VSA. The signal-to-noise ratio of each node of the system is quantitatively calculated in each subsystem model. The output signal-to-noise ratio after processing the bandwidth through the VSA can be expressed by the following formula:

$$\text{SNR}_{\text{VSA}} = \text{SNR}_{\text{link}} + 10\lg \left(\frac{f_s}{2B_{\text{VSA}}} \right), \quad (9)$$

where B_{VSA} is the processing bandwidth of the VSA and SNR_{link} is the link signal-to-noise ratio under the condition of the sampling frequency of f_s . When the above signal-to-noise ratios are all in linear units, as shown in the following formula,

$$\frac{1}{\text{SNR}_{\text{link}}} = \frac{1}{\text{SNR}_{\text{VSG}}} + \frac{1}{\text{SNR}_{\text{jn,ADC}}} + \frac{1}{\text{ANR}_{\text{qn,ADC}}} + \frac{1}{\text{SNR}_{\text{OL}}} + \frac{1}{\text{SNR}_{\text{DAC}}}. \quad (10)$$

Introducing %EVM_{RMS} and PAR, SNR_{VSA} can be expressed by the following formula:

$$\text{SNR}_{\text{VSA}} = -20\lg \left(\frac{\% \text{EVM}_{\text{RMS}}}{100} \right) - 10\lg(\text{PAR}). \quad (11)$$

The system error vector amplitude is obtained, as shown in the following formula:

$$\% \text{EVM}_{\text{RMS}} = 100 \times 10^{[\text{SNR}_{\text{VSA}} + 10\lg(\text{PAR})]/(-20)}. \quad (12)$$

Based on the construction of the intelligent optical fiber network, the microwave is regarded as the load carrier. First, the signal received by the central site is transmitted to the optical carrier through a certain modulation and demodulation, and the intelligent optical fiber is used for transmission to make the signal be detected by the detector at the terminal in the base station and received and transmitted further through portable antenna. The technology of intelligent optical fiber provides long-distance wireless access for radio frequency signals, as shown in Figure 2. For microwave signals that have been modulated and demodulated, the intelligent microwave system is a carrier, a carrier of microwave, and can realize different carrier frequency adjustment. Because each network intelligence is concentrated in the central station, the transmission ratio control of each independent area signal can be realized through each central station, which not only simplifies the construction of the base station but also reduces the power consumption and cost of the entire system and facilitates the system upgrading and maintenance.

2.6. *Typical WOBAN Network Composition.* For the traditional WOBAN network, its characteristic is a tree-like structure. Its core is to use the central site to connect with the routing. The subrouters are used by multiterminal through I-fiber transmission signal to distribute the signals to each back end. The end is composed of corresponding routes to form a network to achieve acquisition, transmission, and response of data.

In turn, any user can use the gateway to reach the back end and realize the spread. Through the use of multipoint control protocol, data transmission is realized, and the corresponding data are discarded to realize efficient and rapid response.

2.7. *Reconfigurable Optical Wireless Network Structure.* The optical wireless network part is another reconfigurable wireless network that is different from the above typical structure. It is a wireless mesh composed of multiple routes and multiple gateways. It is calculated based on the real-time

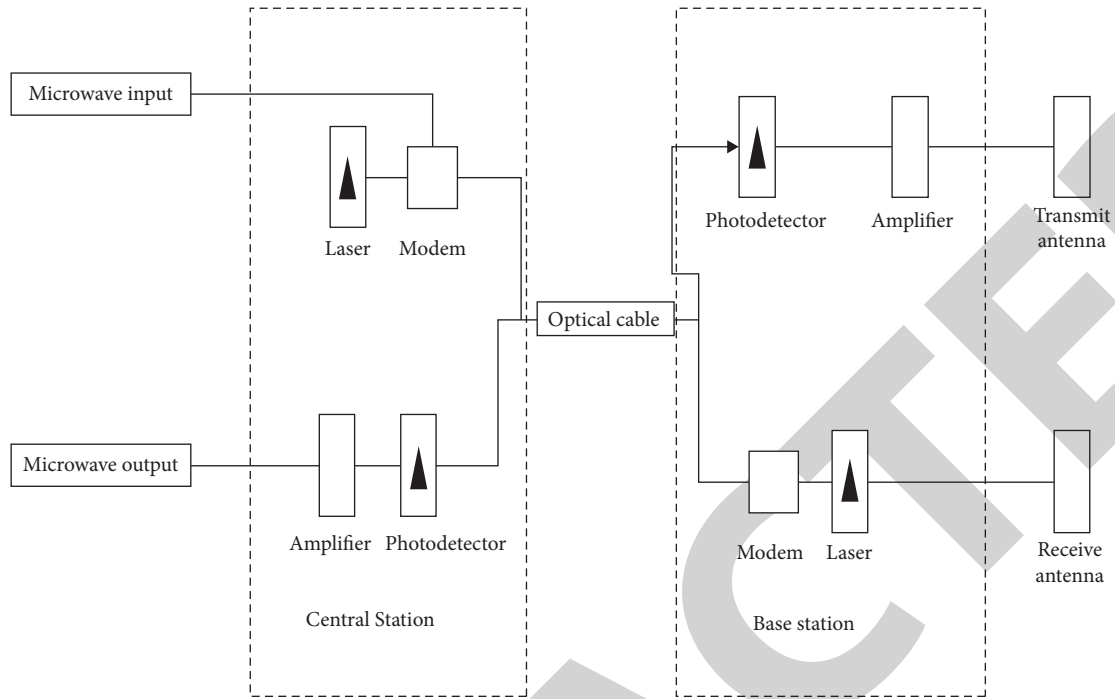


FIGURE 2: Basic concept of ROF technology.

status. Compared with the above typical structure, its structure can realize grid-based efficient management, make more effective use of optical fiber resources, and achieve stronger self-upgrading and maintenance capabilities.

3. Differential Evolution Algorithm

For the differential evolution algorithm (Algorithm 1), its characteristic is a global optimization algorithm, which uses search to perform a global search and achieves the optimal solution through crossover, compilation, and selection. The specific calculation process is as follows.

4. Key Technology Analysis

4.1. Optical Distributed Antenna Technology. For the optical distributed antenna system, it uses smart optical fiber to realize the link between the antenna and the node of the center of gravity. The antenna only needs to complete the conversion between the optical signal and the electrical signal and does not need to care about modulation and demodulation, but with the increase of the amount of data, the antenna system needs to complete the photoelectric signal conversion more efficiently, which puts forward higher requirements on the antenna technology. Therefore, in terms of research, through the realization of distributed antenna simulation, the optical signal is distributed to different terminal antennas and is processed in a distributed manner at the same time to achieve high efficiency of the effectiveness and time and to meet the centralized management of the system [14, 15].

```

Input: population:  $M$ ; crossed factor:
 $D$ ; number of iterations  $T$ 
 $t \leftarrow 1$ 
for  $i=1$  to  $M$  do
for  $j=1$  to  $D$  do
 $x_{i,t}^j = x_{\min}^j + \text{rand}(0, 1) * (x_{\max}^j - x_{\min}^j)$ ;
end
end
while ( $|f(\Delta)| > \epsilon$ ) or ( $t \leq T$ ) do
for  $i=1$  to  $M$  do
 $\Rightarrow$  (Mutation and Crossover)
for  $j=1$  to  $D$  do
 $v_{i,t}^j = \text{Mutation}(x_{i,t}^j)$ ;
 $u_{i,t}^j = \text{Crossover}(x_{i,t}^j, v_{i,t}^j)$ ;
end
 $\Rightarrow$  (Selection)
if then
if  $f(u_{i,t}) < f(x_{i,t})$  then
 $x_{i,t} \leftarrow u_{i,t}$ ;
if  $f(x_{i,t}) < f(\Delta)$  then
 $\Delta \leftarrow x_{i,t}$ ;
end
else
 $x_{i,t} \leftarrow x_{i,t}$ ;
end
end
 $t = t + 1$ 
end
return the best  $\Delta$ 

```

ALGORITHM 1

4.2. Cognitive Radio Technology. For radio technology, it is an improvement technology for the frequency spectrum. For example, the corresponding parameters can be adjusted adaptively to face the complex transmission environment to achieve the double balance of transmission distance and transmission efficiency. On the other hand, it can access the required spectrum autonomously and dynamically according to the results of related perception. For different users and different needs, distributed radio technology is needed to realize the management and adaptive adjustment of optical signals.

4.3. Low-Power Green Smart Optical Fiber Technology. The focus concerned by low-power smart optical fiber technology is to use low-power and low-energy technologies, for reducing network energy consumption, which is of great significance to enterprises, governments, and individuals. Therefore, "green" interconnection not only reduces cost but also reduces energy consumption. The deployment of a large number of terminal devices consumes bandwidth and coverage while also bringing a large amount of consumption. Therefore, the intelligent optical fiber technology required for realization of low power consumption requires optimizing and improving the corresponding routing algorithm. When the power is minimized, the bandwidth can be balanced and the equipment can be accessed in an orderly manner.

5. ROF-Based Automatic Transmission Characteristics of Radio Frequency

5.1. Single-Sideband Transmission Characteristics. For wireless radio frequency automation, a smart optical fiber system for unilateral transmission is chosen in this paper. On the one hand, this can improve the signal attenuation caused by fiber dispersion and increase the distance for effective transmission. On the other hand, compared with the bilateral transmission method, the bandwidth occupied by it is smaller and the cost is lower. According to the principle of unilateral transmission, a corresponding transmission system is constructed in this paper, and corresponding research is conducted on the characteristics of transmission, as shown in Figure 3.

For the corresponding signal generated from radio frequency, the light carrier is realized in the form of light loading through modulator-demodulator. Through long-distance transmission, one part of signal is filtered, while the other part needs to be detected through detector for the transmission condition.

The result of the optical single-sideband signal generated after the filter is shown in Figure 4. Based on the result, the spectrum output contains the signal of the optical carrier and the sideband signal, and the remaining signals have been filtered out. On this basis, the corresponding signal modulation is put on microblog to carry on the quality performance test to the received signal; the error vector value is about 9%; the signal-to-noise ratio is about 20 dB.

5.2. Double-Sideband Carrier Suppressed Transmission Characteristics. The frequency conversion of the photoelectric transmission signal is realized to reduce the adverse effects of the dispersion of the optical fiber in this paper. The specific block diagram is shown in Figure 5:

For the overall system, when the frequency conversion of the carrier signal is realized, the change and conversion of the photoelectric signal are also realized, and the received signal-to-noise ratio is about 24.8%, which can meet the requirements of wireless communication for the quality of related signals.

- (1) According to the above algorithm, the quantitative estimates can be performed effectively for the relationship between the resolution and the signal-to-noise ratio. From the calculation results, when the resolution is less than 6 bits, the quantified signal-to-noise ratio plays a dominant role. On the contrary, when the resolution is greater than 7 bits, the result of link signal-to-noise ratio is equal to the resolution signal-to-noise ratio. Therefore, 8 bits is the corresponding threshold result, and the signal-to-noise ratio result is about 39 dB.
- (2) We calculated the specific relationship between the response link and the bit error rate. The calculated result is as shown in Figure 6. From the results, there is negative correlation between the bit error rate and the optical link. Therefore, when the number of optical links increases, the response bit error rate is effectively reduced.
- (3) The calculation result between the system error vector and the resolution is shown in Figure 7. From the results, it can be seen that when the resolution is less than 7 bits, the system error vector is negatively correlated with the ADC. When the resolution reaches 8 bits, the system error vector and ADC are in an undesirable state, and the value is stable, about 0.7%. Therefore, 8 bits can be regarded as a stable resolution threshold.
- (4) As an important indicator, the signal-to-noise ratio of the system link is determined by the resolution of the ADC. Therefore, in order to study more appropriately, the system error is calculated as the relationship between the important influencing factor and the signal-to-noise ratio. The specific results are shown in Figure 8. From the results, it can be seen that when the signal-to-noise ratio result is less than 35 dB, the system's error vector value is negatively correlated with the signal-to-noise ratio; on the contrary, when the signal-to-noise ratio result is greater than 35 dB, the error vector value of the system has no obvious relationship with the signal-to-noise ratio.

In combination with the above results, it can be seen that the result of the differential evolution algorithm can make the ADC resolution reach 8 bits, which effectively realizes the optimization of the system signal-to-noise ratio. When the signal-to-noise ratio of the system chain is determined by

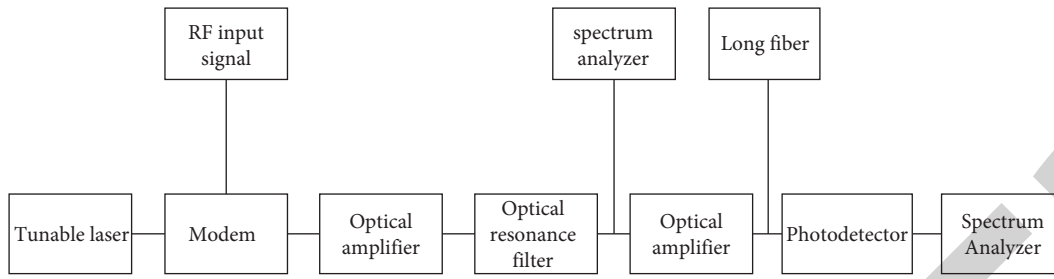


FIGURE 3: Long optical fiber microwave optical fiber transmission system.

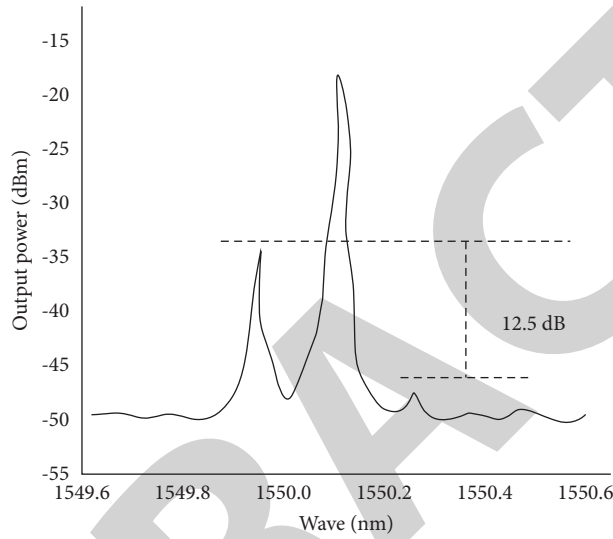


FIGURE 4: Optical single-sideband signal generated through the filter.

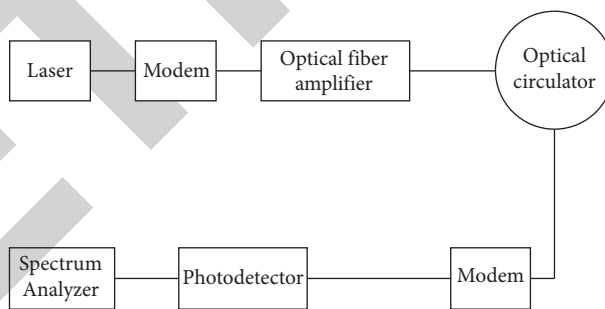


FIGURE 5: System functional block diagram based on double-sideband carrier suppression.

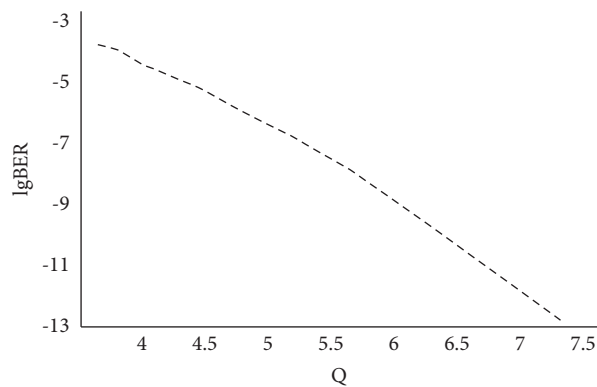


FIGURE 6: The relationship between BER and Q.

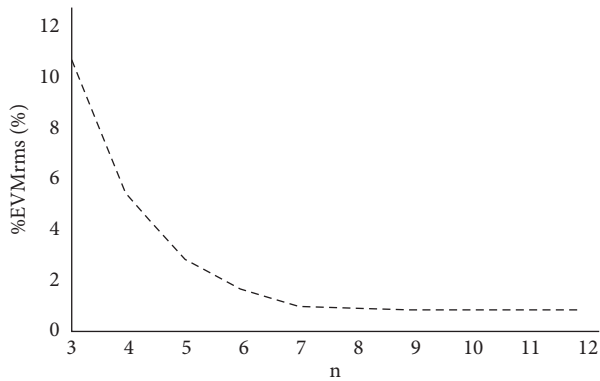


FIGURE 7: The relationship between %EVMRMS and n .

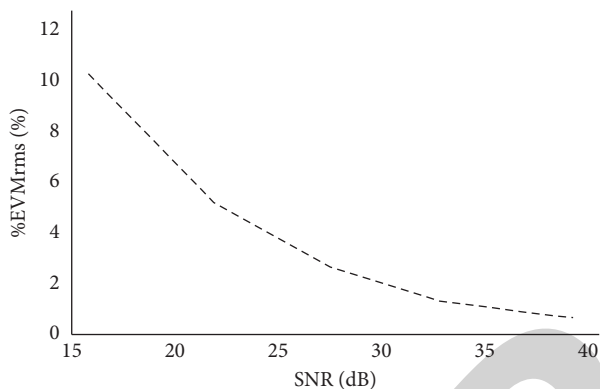


FIGURE 8: The relationship between %EVMRMS and SNRlink.

the system error and the calculated result reaches 36 dB, the optimal error value is about 0.7%, which proves the superiority of the differential evolution algorithm and can effectively support the wireless radio frequency automation of the intelligent optical fiber transmission system.

6. Conclusions

The development of smart optical fiber has given birth to more wireless radio frequency automation technology developments. In view of performance evaluation and other requirements, differential evolution algorithm is introduced in this paper for fusion construction through the integration of optical and wireless networks, and the idea of bilateral transmission is proposed, and the quality requirement of demodulated signal is met through photoelectric signal conversion. On this basis, the corresponding intelligent optical fiber system is introduced, which has the characteristics of high efficiency and long transmission distance and realizes further performance optimization and enhancement of wireless communication.

Data Availability

The data used to support the findings of this study are available from the corresponding author upon request.

Conflicts of Interest

The authors declare no conflicts of interest.

Acknowledgments

This research study was sponsored by State Grid Liaoning Province Electric Power Co., Ltd., scientific and technological project. The name of the project is OTN (Optical Transport Network) network performance automatic monitoring and intelligent operation and maintenance of key technology research and application. The project number is 2020YF-38. The authors thank this project for supporting this article.

References

- [1] R. L. Toaff-Rosenstein, M. Velez, and C. B. Tucker, "Technical note: use of an automated grooming brush by heifers and potential for radiofrequency identification-based measurements of this behavior," *Journal of Dairy Science*, vol. 100, no. 10, pp. 8430–8437, 2017.
- [2] F.-R. Kong, Y.-F. Sun, S. Lin et al., "Experimental studies on radiation intensification in gigahertz radio frequency band by subwavelength plasma structures," *IEEE Transactions on Plasma Science*, vol. 45, no. 3, pp. 381–387, 2017.
- [3] Z. Meng, Y. Liu, N. Gao, Z. Zhang, Z. Wu, and J. Gray, "Radio frequency identification and sensing: integration of wireless powering, sensing, and communication for IIoT innovations," *IEEE Communications Magazine*, vol. 59, no. 3, pp. 38–44, 2021.
- [4] O. Pecher, D. M. Halat, J. Lee et al., "Enhanced efficiency of solid-state NMR investigations of energy materials using an external automatic tuning/matching (eATM) robot," *Journal of Magnetic Resonance*, vol. 275, no. 5, pp. 127–134, 2016.
- [5] R. Sinha, "Automated solid set canopy delivery system (SSCDS) for large scale spray application in tree-fruit crops," *Transactions of the American Society of Agricultural and Biological Engineers*, vol. 62, no. 3, pp. 56–64, 2019.
- [6] F. Santoso and S. J. Redmond, "Indoor location-aware medical systems for smart homecare and telehealth monitoring: state-of-the-art," *Physiological Measurement*, vol. 36, no. 10, pp. 53–60, 2015.
- [7] C. Deans, L. Marmugi, S. Hussain et al., "Electromagnetic induction imaging with a radio-frequency atomic magnetometer," *Applied Physics Letters*, vol. 108, no. 10, pp. 1126–1134, 2016.
- [8] G. Maero, C. Shi, R. Pozzoli et al., "Low-power radio-frequency excitation as a plasma source in a Penning–Malmberg trap: asystematic study," *Journal of Plasma Physics*, vol. 81, no. 5, pp. 495–510, 2015.
- [9] T. Kim, J. S. Kim, and S. J. Heo, "Nasal septal abscess developed after radiofrequency cauterization for epistaxis," *Journal of Craniofacial Surgery*, vol. 30, no. 8, pp. 713–718, 2019.
- [10] M. Ricardo, L. Nuno, P. Fa Bio et al., "Two-step RF IC block synthesis with pre-optimized inductors and full layout generation in-the-loop," *IEEE Transactions on Computer-Aided Design of Integrated Circuits and Systems*, vol. 38, no. 4, pp. 989–1002, 2019.
- [11] V. J. Urick, J. F. Diehl, C. E. Sunderman, J. D. McKinney, and K. J. Williams, "An optical technique for radio frequency interference mitigation," *IEEE Photonics Technology Letters*, vol. 27, no. 12, pp. 1333–1336, 2015.
- [12] A. Lasheras, J. G. Etxebarria, A. Maceiras et al., "Radio frequency magnetoelectric effect measured at high temperature," *IEEE Transactions on Magnetics*, vol. 51, no. 7, pp. 1–4, 2015.

- [13] K. Hanaoka, K. Takahashi, and A. Ando, "Reproducibility of a plasma production in a fast- and automatically-controlled radio frequency plasma source," *IEEE Transactions on Plasma Science*, vol. 2, no. 99, pp. 1-5, 2020.
- [14] A. Nassiri, B. Chase, P. Craievich et al., "History and technology developments of radio frequency (RF) systems for particle accelerators," *IEEE Transactions on Nuclear Science*, vol. 63, no. 2, pp. 707-750, 2016.
- [15] G. C. Wiggins, R. Brown, and K. Lakshmanan, "High-performance radiofrequency coils for²³Na MRI: brain and musculoskeletal applications," *NMR in Biomedicine*, vol. 29, no. 2, pp. 96-106, 2016.

RETRACTED